CRYSTAL GROWTH & DESIGN

pubs.acs.org/crystal

Article

Thermodynamic Approach for Estimating the Melting Enthalpy of Cocrystals

Ahmad Alhadid,* Lea Kefalianakis, Alexander Wendler, Sahar Nasrallah, Christian Jandl, Silva M. Kronawitter, Gregor Kieslich, and Mirjana Minceva

Cite This: *Cryst. Growth Des.* 2024, 24, 4770−4780

Read Online

ACCESS | Metrics & More | Article Recommendations | Supporting Information

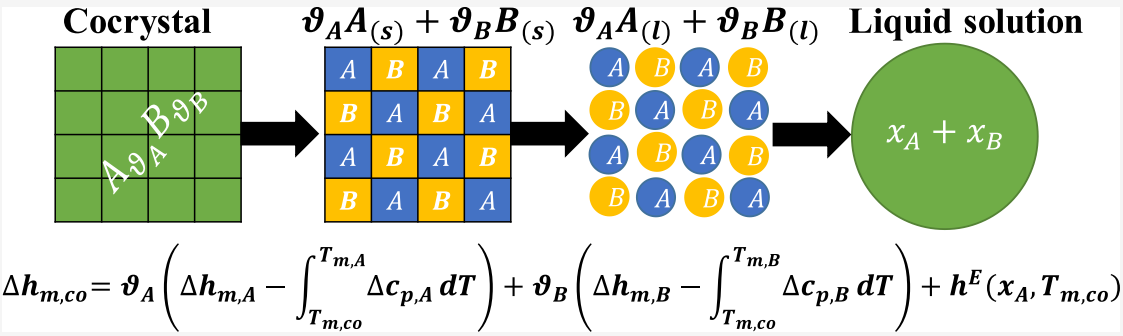

ABSTRACT: The synthesis of cocrystals is an established and efficient method for tuning the solubility of pharmaceutical and industrially relevant compounds. Predicting the cocrystal solubility prerequisites knowledge about the melting properties and the stoichiometry of the cocrystal along with the activity coefficients of individual constituents in the liquid solution. Reliable thermodynamic models can estimate the activity coefficients of components in the liquid phase; on the other hand, predicting the cocrystal melting properties and stoichiometry remains a key challenge. In this work, we propose an approach for estimating the melting enthalpy of cocrystals, where the melting enthalpy of the cocrystal is calculated using the melting properties of its pure constituents, the cocrystal stoichiometry and melting temperature, and the enthalpy of mixing the constituents in the liquid solution. For selected model systems, we show that by using our approach, the calculated melting enthalpy allowed for predicting the cocrystal liquidus line equally well and, in some cases, better than when using the experimental melting enthalpy values. Furthermore, we apply our approach to accurately predict the complete phase diagram of binary eutectic systems with cocrystal formation, in which the properties of the cocrystals have not been reported before. The advantage of our approach is the ability to model the solid−liquid phase diagram of eutectic systems with cocrystal formation without requiring extensive investigations of the cocrystal stoichiometry and melting properties. Therefore, the approach has the capacity to fill gaps of experimental uncertainties in determining the cocrystal melting enthalpy when isolating the cocrystal is challenging. By streamlining the prediction of cocrystal melting enthalpy, our proposed approach could accelerate the identification and design of pharmaceutically active cocrystals, offering a potent tool for expediting drug development processes.

1. INTRODUCTION

Solubility is a property that determines the maximum amount of a substance that can be dissolved in a solution at a specific temperature.[1] The solubility of a solid compound in a solvent at constant temperature depends on its melting properties and activity coefficients in the liquid solution.[2] In many processes, a particular solute can be required to dissolve in a solvent. For instance, the solubility of an active pharmaceutical ingredient in water determines its bioavailability in the human body. Methods for tuning the solubility of compounds rely on altering the melting properties or the activity coefficients of components in the liquid solution.[3] Eutectic mixture formation and hydrotrope addition are exemplary methods used for tuning the activity coefficient of the solute in the liquid solution without altering the solute's melting properties. On the other hand, cocrystal formation allows adjusting the solute's melting properties and activity coefficients in the liquid solution. Cocrystals are solid phases formed by two or more molecular compounds, whereas the cocrystal possesses a crystal structure and melting properties different from that of pure constituents.[4]

Received: March 18, 2024
Revised: May 1, 2024
Accepted: May 3, 2024
Published: May 14, 2024

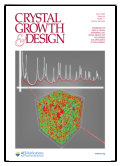

A vast number of components can be used as coformers for cocrystal formation; however, only those improving the solubility should be selected.[3] Modeling solid−liquid equilibria (SLE) can predict the solubility of cocrystals.[5,6] Modeling the solubility of a cocrystal requires its melting properties, stoichiometry, and constituents' activity coefficients in the liquid phase.[7] The activity coefficients of the individual constituents can be calculated using thermodynamic models. Predictive thermodynamic models such as UNIFAC, PC-SAFT, and COSMO-RS can provide a reliable estimate for the activity coefficients of components in the liquid phase.[6,8−16] In contrast, predicting the melting temperature, enthalpy, and stoichiometry of the cocrystal is far more difficult.[17−20] Thus, for modeling the cocrystal solubility, the melting properties of cocrystals should be obtained by thermal analysis (e.g., calorimetry), while solid characterization techniques (e.g., X-ray diffraction) are used to determine the cocrystal stoichiometry. Over 1 million cocrystals are reported in the Cambridge Structure Database (CSD), where the structure, stoichiometry, and, in most cases, melting temperature data are available.[17] Data on the melting enthalpy of these cocrystals are scarcer, which hinders the evaluation of their solubility.

In this work, we propose a thermodynamic approach for estimating the melting enthalpy of cocrystals with known stoichiometry and melting temperature. The approach was used to calculate the melting enthalpy of various cocrystals reported in the literature. Furthermore, the calculated melting enthalpy was used to model the complete SLE phase diagram of binary eutectic systems with cocrystal formation, for which the cocrystal melting properties had not been reported before. The proposed approach would allow for predicting cocrystal solubility without requiring extensive experimental investigations of cocrystal formation.

2. MATERIALS AND METHODS

2.1. Cocrystal Melting Process. The cocrystal is a pure solid, while the melt of the cocrystal is a liquid solution of two components. The melting enthalpy of a cocrystal represents the difference between the enthalpy of the cocrystal in the solid phase and the enthalpy of the liquid solution. In previous works,[7,12,13,21,22] we used the volume of the cocrystal unit cell—estimated from powder X-ray diffraction (PXRD) measurements—and the volume of a pure constituent unit cell to confirm the stoichiometry of the cocrystal. Thus, the cocrystal represents a solid consisting of units of each constituent in the corresponding cocrystal stoichiometric ratio. Figure 1 visualizes the proposed cocrystal melting process. First, the stoichiometric amount of pure solids A and B are melted at the cocrystal melting temperature (i.e., pure solids A and B melt to pure liquids). Second, the two liquids are mixed to form a miscible liquid solution. The enthalpy of mixing the two constituents in the solid state was neglected in this work due to the lack of thermodynamic models that could provide an estimate for this contribution. However, in the case of strong hydrogen bonding interactions, the contribution of enthalpy of mixing the components on the melting enthalpy of the cocrystal should be considered. Previous studies assumed a similar process for the enthalpy of cocrystal formation (i.e., the enthalpy of crystallizing the cocrystal from the liquid solution).[23,24] However, the total enthalpy of cocrystal formation was determined experimentally by thermal analysis. In contrast, we propose a thermodynamic approach in this work to calculate the melting enthalpy of the cocrystal without the need for an extensive experimental investigation.

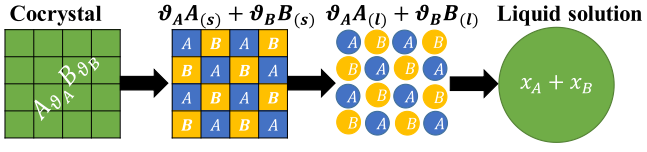

Figure 1. Assumed melting process of the cocrystal. The cocrystal consists of units of components A and B with the corresponding cocrystal stoichiometric ratio. Pure solids A and B melt to form a liquid solution.

2.2. Thermodynamic Cycle. This section explains estimating the enthalpy change in the cocrystal melting process assumed in this work (Figure 1). A cocrystal formation is described according to the following reaction

$$\vartheta_A A_{(L)} + \vartheta_B B_{(L)} \leftrightarrow A_{\vartheta_A} B_{\vartheta_B(S)} \tag{1}$$

where ϑ_A and ϑ_B are the stoichiometric coefficients of components A and B in the cocrystal, respectively. The cocrystal consists of ϑ_A moles of A and ϑ_B moles of B, which melt at the cocrystal melting temperature and are mixed to form a liquid solution. The following equation describes the total enthalpy change of the cocrystal melting process ($\Delta h_{m,\mathrm{co}}$) at the cocrystal melting temperature ($T_{m,\mathrm{co}}$), neglecting the enthalpy of mixing the components in the solid phase

$$\Delta h_{m,\mathrm{co}}(T_{m,\mathrm{co}}) = \vartheta_A \Delta h_{m,A}(T_{m,\mathrm{co}}) + \vartheta_B \Delta h_{m,B}(T_{m,\mathrm{co}}) + h^E(x_{A,\mathrm{co}}, T_{m,\mathrm{co}}) \tag{2}$$

where Δh_m is the melting enthalpy of pure components, h^E is the enthalpy of mixing, and $x_{A,\mathrm{co}}$ is the mole fraction of component A in the cocrystal melt, which is calculated as follows

$$x_{A,\mathrm{co}} = \frac{\vartheta_A}{\vartheta_A + \vartheta_B} \tag{3}$$

The first two terms on the right-hand side of eq 2 depend on the melting properties of pure components, their stoichiometric ratio in the cocrystal, and the melting temperature of the cocrystal. The enthalpy change of melting pure components A and B at the cocrystal melting temperature is inaccessible. A thermodynamic cycle similar to that used to model SLE was constructed to estimate the melting enthalpy of pure components at the cocrystal melting temperature. Figure 2 shows the thermodynamic cycle used to estimate the melting enthalpy of pure components A (left cycle) and B (right cycle) at the melting temperature of the cocrystal ($T_{m,\mathrm{co}}$). First, pure solids A and B are heated or cooled from the cocrystal melting temperature ($T_{m,\mathrm{co}}$) to the melting temperatures of pure components A and B ($T_{m,A}$ and $T_{m,B}$, respectively), and the enthalpy change ($\Delta h_{1\to 2}$) is calculated as follows

$$\Delta h_{\vec{1}\to 2} = \int_{T_{m,\mathrm{co}}}^{T_{m,i}} c_{p,i}^{S}\, \mathrm{d}T \tag{4}$$

where c_p^s is the constant pressure heat capacity of pure solids A and B. After that, pure solids A and B melt at their respective melting temperatures; hence, the enthalpy change in this step ($\Delta h_{2\to 3}$) equals the melting enthalpy of pure components A and B ($\Delta h_{m,A}$ and $\Delta h_{m,B}$, respectively). Finally, the pure liquids A and B are cooled or heated from their melting temperatures to the cocrystal melting temperature, and the enthalpy change is calculated as follows

$$\Delta h_{\vec{3}\to 4} = \int_{T_{m,i}}^{T_{m,\mathrm{co}}} c_{p,i}^{L}\, \mathrm{d}T \tag{5}$$

where c_p^L is the constant pressure heat capacity of pure liquids A and B. Summing the enthalpy changes along the path ($\Delta h_{1\to 2} + \Delta h_{2\to 3} + \Delta h_{3\to 4}$), eq 2 becomes

$$\Delta h_{m,\mathrm{co}} = \vartheta_A\left(\Delta h_{m,A} - \int_{T_{m,\mathrm{co}}}^{T_{m,A}} \Delta c_{p,A}\, \mathrm{d}T\right) + \vartheta_B\left(\Delta h_{m,B} - \int_{T_{m,\mathrm{co}}}^{T_{m,B}} \Delta c_{p,B}\, \mathrm{d}T\right) + h^E(x_A, T_{m,\mathrm{co}}) \tag{6}$$

https://doi.org/10.1021/acs.cgd.4c00393
Cryst. Growth Des. 2024, 24, 4770−4780

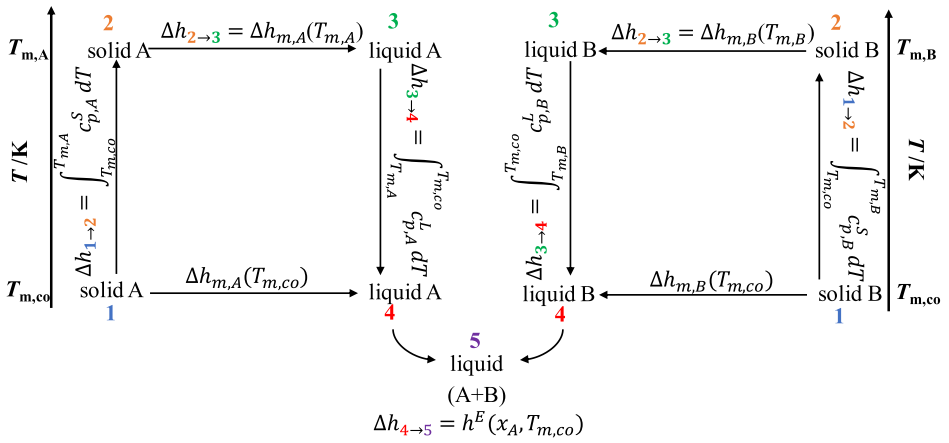

Figure 2. Thermodynamic cycle for estimating the melting enthalpy of a cocrystal.

where $\Delta c_p = c_p^L - c_p^s$. In case a pure component undergoes a solid−solid transition, the solid−solid transition enthalpy should be considered when calculating its melting enthalpy.

The third term on the right-hand side of eq 6 is the enthalpy of mixing ($\Delta h_{4\to5} = h^E$), which can readily be calculated using excess Gibbs energy (g^E) models according to the following thermodynamic relation

$$\left(\frac{\partial g^E/T}{\partial T}\right)_{p,x} = -\frac{h^E}{T^2} \tag{7}$$

2.3. Thermodynamic Modeling. The SLE phase diagram of binary eutectic systems with cocrystal formation can be constructed by calculating the liquidus lines of the pure constituents and cocrystals. The liquidus line of pure component i is calculated as follows[2]

$$\ln(x_i\gamma_i) = \frac{\Delta h_{m,i}}{RT}\left(\frac{T}{T_{m,i}} - 1\right) + \frac{1}{RT}\int_{T_{m,i}}^{T} \Delta c_{P,i}\, dT - \frac{1}{R}\int_{T_{m,i}}^{T} \frac{\Delta c_{P,i}}{T}\, dT \tag{8}$$

where γ is the activity coefficient of component i in the liquid phase, T is the liquidus temperature, and R is the universal gas constant. For components undergoing a solid−solid transition, the liquidus line below the solid−solid transition temperature is calculated as follows[11]

$$\ln(x_i\gamma_i) = \frac{\Delta h_{m,i}}{RT}\left(\frac{T}{T_{m,i}} - 1\right) + \frac{\Delta h_{tr,i}}{RT}\left(\frac{T}{T_{tr,i}} - 1\right) + \frac{1}{RT}\left(\int_{T_{tr,i}}^{T} \Delta c_{p,i}^{L\to S1}\, dT + \int_{T_{m,i}}^{T_{tr,i}} \Delta c_{p,i}^{L\to S2}\, dT\right) - \frac{1}{R}\left(\int_{T_{tr,i}}^{T} \frac{\Delta c_{p,i}^{L\to S1}}{T}\, dT + \int_{T_{m,i}}^{T_{tr,i}} \frac{\Delta c_{p,i}^{L\to S2}}{T}\, dT\right) \tag{9}$$

where Δh_{tr} and $T_{tr,i}$ are the solid−solid transition enthalpy and temperature, respectively, and $\Delta c_{p,i}^{L\to S1} = \Delta c_{p,i}^{L} - \Delta c_{p,i}^{S1}$ and $\Delta c_{p,i}^{L\to S2} = \Delta c_{p,i}^{L} - \Delta c_{p,i}^{S2}$.

The cocrystal liquidus line was calculated using the equilibrium constant of the cocrystal formation reaction (eq 1) as follows[7]

$$\ln K_a(x, T) = \ln K_a(x_{A,co}, T_{m,co}) + \frac{\Delta h_{m,co}}{R}\left(\frac{1}{T_{m,co}} - \frac{1}{T}\right) \tag{10}$$

$$K_a = (x_A\gamma_A)^{\vartheta_A}(x_B\gamma_B)^{\vartheta_B} \tag{11}$$

where $x_{A,co}$ can be calculated by eq 3.

The activity coefficients of components in the liquid solution can be calculated using various thermodynamic models. Correlative activity coefficient models could accurately describe the nonideality of various eutectic systems with cocrystal formation.[7,12] In this work, we used the nonrandom two-liquid (NRTL) equation to calculate the activity coefficients of components as follows[2]

$$\ln\gamma_i = x_j^2\left[\tau_{ji}\left(\frac{G_{ji}}{x_i + x_jG_{ji}}\right)^2 + \frac{\tau_{ij}G_{ij}}{(x_j + x_iG_{ij})^2}\right] \tag{12}$$

$$G_{ij} = \exp(-\alpha\tau_{ij}) \qquad G_{ji} = \exp(-\alpha\tau_{ji}) \tag{13}$$

$$\tau_{ij} = \frac{g_{ij} - g_{jj}}{RT} \qquad \tau_{ji} = \frac{g_{ji} - g_{ii}}{RT} \tag{14}$$

Due to the limited experimental data in some systems, only the system-specific binary interaction parameters $(g_{ij} - g_{jj})$ and $(g_{ji} - g_{ii})$ were obtained by fitting the experimental liquidus temperatures of pure components. On the other hand, a typical value of 0.3 was assumed for the nonrandomness parameter (α).[2] The root-mean-square deviation (RMSD) between experimental and calculated liquidus temperatures was used as an objective function

$$\text{OF} = \text{RMSD} = \left(\frac{\sum_{i=1}^{n}(T_i^{exp} - T_i^{cal})^2}{n}\right)^{1/2} \tag{15}$$

The enthalpy of mixing (h^E) is calculated using the NRTL model as follows[25]

$$h^E = \left(\frac{x_ix_jG_{ji}}{(x_i + x_jG_{ji})}\right)\left(1 - \frac{\alpha\tau_{ji}x_i}{(x_i + x_jG_{ji})}\right)(g_{ji} - g_{ii}) + \left(\frac{x_ix_jG_{ij}}{(x_j + x_iG_{ij})}\right)\left(1 - \frac{\alpha\tau_{ij}x_j}{(x_j + x_iG_{ij})}\right)(g_{ij} - g_{jj}) \tag{16}$$

2.4. Systems Selection. According to eq 6, the melting enthalpy of a cocrystal can be calculated using the melting properties of pure constituents, the heat capacity of pure solid and liquid states, and the enthalpy of mixing. Thus, to evaluate the proposed approach in calculating the cocrystal melting enthalpy, systems with available SLE data and whose components' melting properties and heat capacity are known were selected in this study. Table S1 in the Electronic Supporting Information shows the selected systems and the stoichiometry and melting temperature of the cocrystals in each system. The pure components' properties used for SLE modeling are available in Tables S2−S4 in the Electronic Supporting Information. It should be noted that the linear temperature dependency of constant pressure heat capacity of solid and liquid states was assumed, and the coefficients of the linear functions obtained in this work can be found

https://doi.org/10.1021/acs.cgd.4c00393
Cryst. Growth Des. 2024, 24, 4770−4780

in Table S3. However, for some components, namely, 3,4-xylenol, 3,5-xylenol, and choline chloride (ChCl), no temperature-dependent heat capacity data are available in the literature. Thus, a constant Δc_p value reported in the literature was used, which was estimated from the difference between the heat capacity of the solid and liquid at the melting temperature of the component.

Moreover, to ensure a reliable estimate of the enthalpy of mixing in each system, the NRTL model was applied (eq 16). The NRTL binary interaction parameters were obtained by fitting the experimental SLE data of pure components liquidus lines. Table S5 in the Electronic Supporting Information shows the NRTL binary interaction parameters of the studied systems obtained in this work or found in the literature.

Partial miscibility in the solid phase was observed in the thymol/L-menthol system, and the liquidus lines of thymol and 1:3 thymol/L-menthol could not be modeled using eqs 8 and 10, respectively. Details about the modeling procedure of SLE in the thymol/L-menthol system can be found in the original paper.[22]

2.5. SLE Measurements. The SLE data of the binary systems ChCl/resorcinol and nicotinamide/glutaric acid, as well as the 1:2 ChCl/urea cocrystal melting properties, were measured in this work. Table 1 shows the pure components used to prepare the eutectic mixtures, along with their purity and source. ChCl was dried before being used for 24 h at 353 K and 1 Pa, and the water content was checked (<500 ppm) using a Karl Fischer Coulometer (Hanna Instruments). The other components were used as received without further purification.

Table 1. Chemicals Used to Prepare Eutectic Systems and Cocrystals

substance	declared purity	source
ChCl	>98%	Alfa Aesar
resorcinol	99%	Alfa Aesar
urea	>99%	Sigma-Aldrich
nicotinamide	99.5%	Sigma-Aldrich
glutaric acid	99%	Thermo Fisher Scientific

The mixtures were prepared by weighting (precision 0.1 mg, max 150 g) and mixing the pure components in various ratios inside hermetically sealed glass vials until a clear homogeneous liquid was obtained. For the ChCl/resorcinol and ChCl/urea systems, the samples were quenched at 193 K and then stored at 253 K until crystallization of the samples was observed. On the other hand, the nicotinamide/glutaric acid system samples were crystallized at room temperature.

Differential scanning calorimetry (DSC) (NETZSCH DSC 200 F3) was used to measure the liquidus and solidus temperatures as well as the melting temperature of pure components and cocrystals. Details about the DSC measurements and the experimental SLE data can be found in the Electronic Supporting Information (Tables S6 and S7).

Cocrystal formation was investigated using PXRD, which revealed the formation of 1:1 and 1:2 ChCl/resorcinol, 1:2 ChCl/urea, and 1:1 nicotinamide/glutaric acid cocrystals. Details about the PXRD measurements and the experimental results can be found in the Electronic Supporting Information (Figures S1−S3).

3. RESULTS

The proposed approach for calculating the cocrystal melting enthalpy was applied to 24 different cocrystals formed in 15 different eutectic systems found in the literature or measured in this work. The systems were categorized into two groups. The first group comprises 10 binary eutectic systems containing 15 cocrystals with known melting properties and stoichiometry. Accordingly, these systems were used to evaluate the approach proposed in this work by directly comparing the calculated and experimental melting enthalpy values and modeling the cocrystal liquidus lines using predicted and experimental melting enthalpies. The second group consists of 6 binary eutectic systems containing 9 cocrystals, where the cocrystal formation was not investigated and was only speculated by the course of experimental SLE data. The predicted melting enthalpy of the cocrystals in these 6 binary systems was evaluated by modeling the liquidus lines of the cocrystal in each eutectic system.

3.1. Systems with Known Cocrystal Melting Enthalpy. In this section, the approach was applied to 10 binary eutectic systems, where cocrystal formation was extensively studied by thermal and solid-phase analyses. The cocrystal melting enthalpy was calculated by eq 6 using the experimental melting temperature and stoichiometry of cocrystals; Table 2 shows the predicted melting enthalpy of the cocrystals compared to the experimental ones. As can be seen in Table 2, the predicted melting enthalpy values agreed with the experimental ones in some cases, while a significant deviation could be observed in others. It is important to point out here

Table 2. Comparison between Experimental and Predicted Melting Enthalpy of the Studied Cocrystal Systems[a]

component 1	component 2	cocrystal ratio	$T_{m,co}$/K	$\Delta h_{m,co}^{exp}$/kJ mol^{-1}	$\Delta h_{m,co}^{cal}$/kJ mol^{-1}	Δ/%[b]
l-menthol[12]	phenol	1:2	273.3	27.48	28.53	3.8
		2:1	269.4	20.35	28.66	40.8
thymol[22]	L-menthol	3:1	285.7	45.0	63.7	41.5
		2:3	274.7	44.90	63.89	42.3
3,4-xylenol[13]	L-menthol	2:1	299.7	45.71	41.22	−9.8
		1:2	289.3	37.95	37.03	−2.4
3,5-xylenol[13]	L-menthol	1:1	287.5	21.51	27.51	27.9
urea[29]	phenol	1:2	332.7	59.77	40.74	−31.8
nicotinamide[c]	glutaric acid	1:1	409.7	54.62 ± 0.9	48.66	−10.9
ChCl[7]	catechol	1:2	325.7	39.54	54.71	38.4
		1:1	327.4	34.15	36.18	5.9
ChCl[c]	resorcinol	1:2	300.1	24.0 ± 0.1	44.17	84.0
		1:1	301.6	18.23 ± 0.2	30.26	66.0
ChCl[7]	hydroquinone	1:1	332.7	31.97	36.72	14.9
ChCl	urea	1:2	298.1[c]	25.86 ± 0.5[c]	42.20	63.2
			297.7[30]	24.30[30]		73.7

[a]The cocrystal ratio was determined via single-crystal or PXRD. [b]$\Delta = \frac{\Delta h_{m,co}^{cal} - \Delta h_{m,co}^{exp}}{\Delta h_{m,co}^{exp}} \times 100\%$. [c]Measured in this work.

https://doi.org/10.1021/acs.cgd.4c00393
Cryst. Growth Des. 2024, 24, 4770−4780

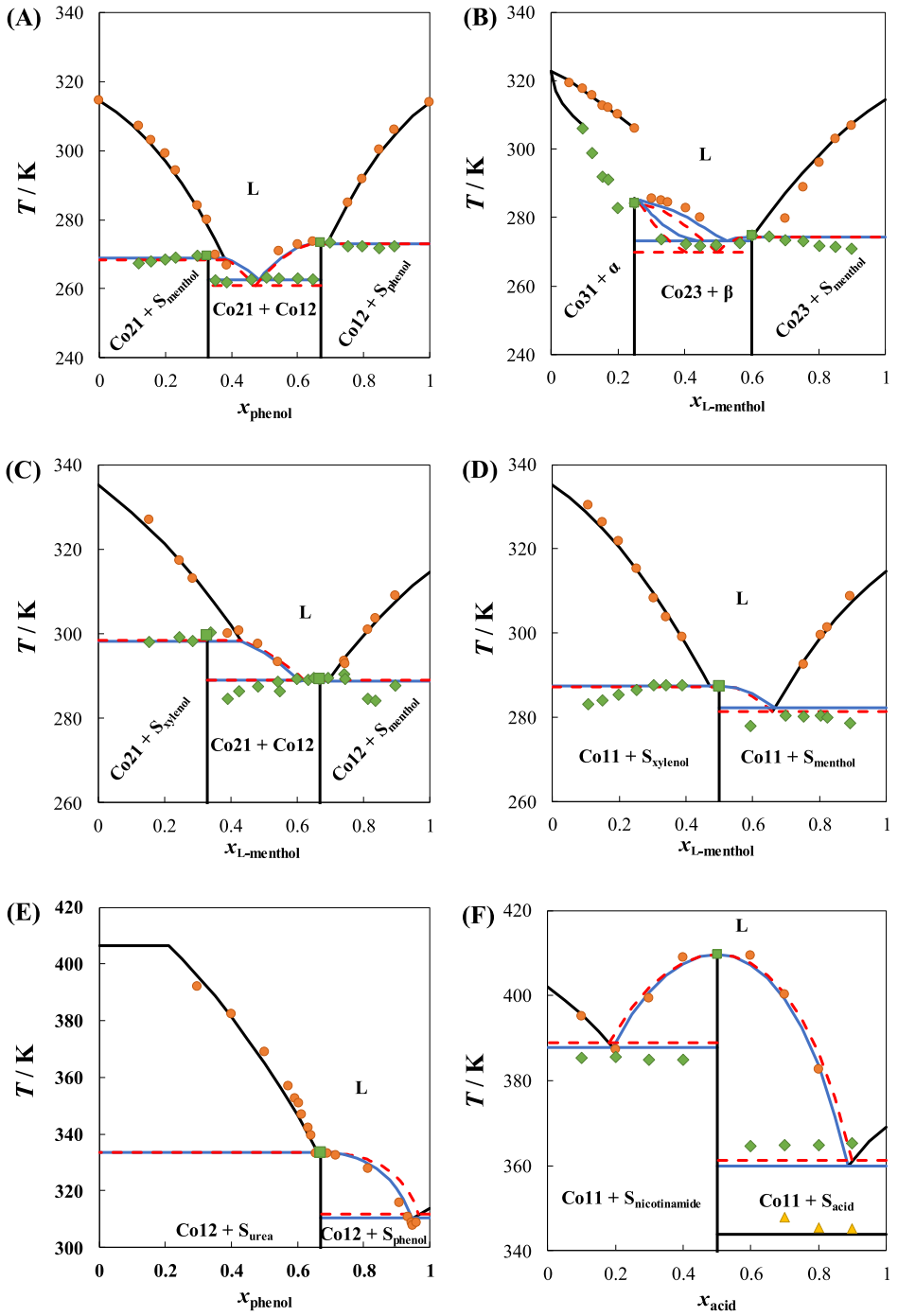

Figure 3. Solid−liquid phase diagram of (A) L-menthol/phenol,[12] (B) thymol/L-menthol,[22] (C) 3,4-xylenol/L-menthol,[13] (D) 3,5-xylenol/L-menthol,[13] (E) urea/phenol,[28] and (F) nicotinamide/glutaric acid. Legend: ● (orange) liquidus data; ◆ (green) solidus data; ■ (green) cocrystal; ▲ (yellow) solid−solid transition; —— NRTL; —— (blue) calculated using $\Delta h_{m,co}^{cal}$; and ---- (red) calculated using $\Delta h_{m,co}^{exp}$.

that the deviation was higher in predicting the melting enthalpy of incongruently melting cocrystals (e.g., 2:1 L-menthol/phenol, 3:1 thymol/L-menthol, and 1:2 urea/phenol) or those that were difficult to crystallize (e.g., ChCl/urea 1:2 and 2:3 thymol/L-menthol). For instance, the relative deviation between the experimental and predicted melting enthalpy of the 1:1 (Δ = 66%) and 1:2 (Δ = 84%) ChCl/resorcinol cocrystals was relatively large. The DSC curve of the 1:1 ChCl/resorcinol cocrystal showed two adjacent peaks (see Figure S4 in the Electronic Supporting Information). Variable-temperature PXRD measurements did not indicate any solid−solid transition up to the melting temperature (see Figure S5 in the Electronic Supporting Information). Thus, it was difficult to interpret the DSC curve and determine the melting enthalpy of the 1:1 ChCl/resorcinol cocrystal. On the other hand, the 1:2 ChCl/resorcinol cocrystal could only be partially crystallized after several weeks of storing at 253 K. The melting peak of the 1:2 ChCl/resorcinol cocrystal in the DSC curve was broad and asymmetrical, indicating that the solid phase could be inhomogeneous (see Figure S4 in the Electronic Supporting Information), and the measured melting enthalpy might be underestimated. Measuring the melting enthalpy of incon-

https://doi.org/10.1021/acs.cgd.4c00393
Cryst. Growth Des. 2024, 24, 4770−4780

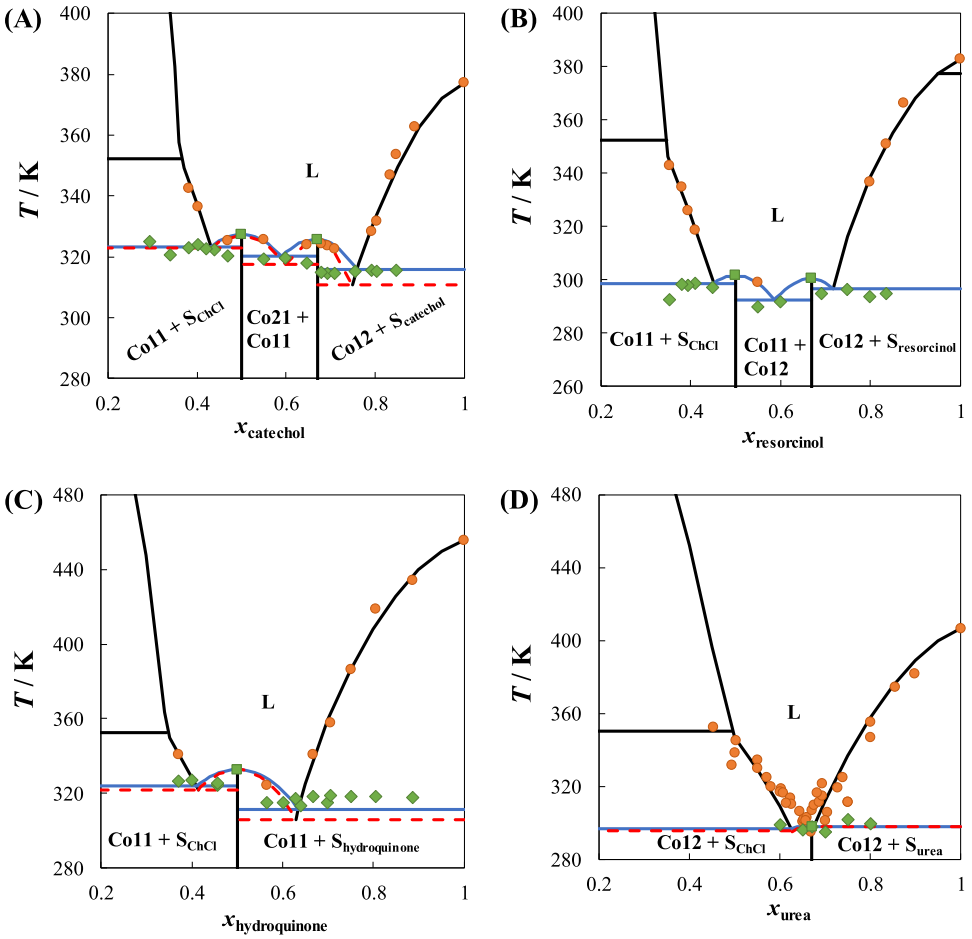

Figure 4. Solid−liquid phase diagram of (A) ChCl/catechol,[7] (B) ChCl/resorcinol, (C) ChCl/hydroquinone,[7] and (D) ChCl/urea.[30,35,37] Legend: ● (orange) liquidus data; ◆ (green) solidus data; ■ (green) cocrystal; —— NRTL; —— (blue) calculated using $\Delta h_{m,co}^{cal}$; and ----- (red) calculated using $\Delta h_{m,co}^{exp}$.

gruently melting cocrystals or cocrystals with kinetically hindered crystallization might be challenging.[22] Accordingly, the experimental melting enthalpy of some cocrystals in Table 2 is expected to have large uncertainties.

Furthermore, the uncertainty of the heat capacity values might also influence the predicted melting enthalpy values. Pure solid or liquid states' heat capacity is unavailable for some compounds. For instance, only the difference in heat capacity at the melting temperature was reported for ChCl,[26,27] 3,4-xylenol, and 3,5-xylenol.[28] Thus, without reliable data on the heat capacity of the solid and liquid states of pure components, the approach might not accurately predict the melting enthalpy of the cocrystals.

Due to the difficulty of measuring the melting enthalpy of some cocrystals and the lack of experimental data on the heat capacity of some pure components, comparing the predicted and experimental melting enthalpy values might not allow for a fair evaluation of the approach. Therefore, we chose an alternative for benchmarking the predicted melting enthalpy values by comparing the calculated liquidus lines of cocrystals in the studied eutectic systems using the experimental and predicted melting enthalpy values. Figure 3 shows the SLE phase diagram of 6 binary eutectic systems where the liquidus line of cocrystals was calculated using the predicted and experimental melting enthalpies. As can be seen in Figure 3A, because the predicted melting enthalpy of the 1:2 L-menthol/phenol cocrystal was in good agreement with the experimental values, the liquidus lines calculated using the predicted and experimental melting enthalpy values were similar and in good agreement with the measured SLE data of the cocrystals. In contrast, despite the large deviation between the predicted and experimental melting enthalpy of the 2:1 L-menthol/phenol cocrystal, the predicted melting enthalpy of the cocrystal better described the solidus temperature of the system in the middle composition range. As can be seen in Figure 3B, the predicted melting enthalpy of the 3:1 thymol/L-menthol cocrystal allowed for a better description of the SLE data of the cocrystal compared to the experimental melting enthalpy. Due to the narrow composition range of the 2:3 thymol/L-menthol cocrystal liquidus line, it was impossible to differentiate between the liquidus lines calculated using experimental and predicted melting enthalpy values; however, the eutectic temperature of the system in the middle section of the phase diagram was better estimated using the calculated melting enthalpy than using the experimental one. Despite the deviation between the predicted and experimental melting enthalpy values of the cocrystals formed in the binary mixture of L-menthol with 3,4-xylenol (Figure 3C) and 3,5-xylenol (Figure 3D), the liquidus lines calculated using the experimental and predicted melting enthalpy values were similar and allowed for a good description of the SLE data of the cocrystals. In contrast, for the urea/phenol system (Figure

https://doi.org/10.1021/acs.cgd.4c00393
Cryst. Growth Des. 2024, 24, 4770−4780

3E), the predicted melting enthalpy allowed for a better description of the SLE data of the 1:2 urea/phenol cocrystal, where the liquidus line calculated using the experimental melting enthalpy of the cocrystal largely deviated from the experimental SLE data. In conclusion, the proposed approach allowed for a good description of SLE data of cocrystals, filling gaps of experimental uncertainties when measuring the cocrystal melting enthalpy was challenging.

Besides applying the approach to literature data, the approach was used to estimate the cocrystal melting enthalpy of the nicotinamide/glutaric acid system measured in this work. Nicotinamide is a well-known pharmaceutical coformer, which was found to induce a negative deviation from ideality when mixed with carboxylic acids.[23,31] Glutaric acid is a stable dicarboxylic acid with well-characterized melting properties.[32,33] The SLE phase diagram of the nicotinamide/glutaric acid system was measured in this work, and the results are shown in Figure 3F. The measured SLE phase diagram suggested the formation of a 1:1 nicotinamide/glutaric acid cocrystal, confirmed by PXRD measurements (see Figure S3 in the Electronic Supporting Information). Due to the lack of liquidus data for glutaric acid, the NRTL binary interaction parameters were obtained by fitting the cocrystal liquidus data. Nevertheless, the predicted melting enthalpy of the cocrystal calculated using eq 6 and the enthalpy of mixing calculated by NRTL (eq 16) were used to model the SLE data of the cocrystal. As can be seen in Figure 3F, both predicted and experimental melting enthalpy of the cocrystal could well describe the SLE data of the 1:1 nicotinamide/glutaric acid cocrystal.

Next, the approach was applied to predict the melting enthalpy of the cocrystals formed in 4 eutectic systems containing ChCl, namely, ChCl/catechol,[7] ChCl/resorcinol, ChCl/hydroquinone,[7] and ChCl/urea. Many ChCl-based eutectic systems, commonly known as deep eutectic solvents, show significant negative deviation from ideality.[34] ChCl was found to form cocrystals with the two dihydroxybenzene isomers, namely, catechol and hydroquinone.[7] In this work, SLE in the ChCl/resorcinol system—the third dihydroxybenzene isomer—was investigated. At the time of investigating the SLE in ChCl/catechol and ChCl/hydroquinone in our previous work,[7] ChCl melting properties were not available, as ChCl decomposes before melting. Thus, the SLE data of the cocrystals were fitted to obtain the NRTL binary interaction parameters in ChCl-based eutectic systems with cocrystal formation using the experimental melting properties of the cocrystals.[7,21] Recently, van den Bruinhorst et al.[26] overcame ChCl decomposition before melting by fast scanning calorimetry allowing for measuring ChCl melting properties. Here, the NRTL binary interaction parameters of ChCl/catechol and ChCl/hydroquinone could be obtained by fitting pure components' liquidus data. The binary interaction parameters of the ChCl/catechol and ChCl/hydroquinone systems obtained in this work agreed with those obtained by fitting the cocrystal liquidus data (see Table S5 in the Electronic Supporting Information). The agreement between the binary interaction parameter obtained from the two methods implies the reliability of the measured melting properties of ChCl and the approach to estimate the nonideality of thermally unstable substances utilizing cocrystal formation.

As can be seen in Table 2, the predicted melting enthalpy of the 1:1 ChCl/catechol cocrystal agreed with the experimental melting enthalpy of the cocrystal. Accordingly, the liquidus line of the 1:1 ChCl/catechol cocrystal calculated by using the predicted and experimental melting enthalpy values was similar and in good agreement with the experimental SLE data. In contrast, the predicted melting enthalpy of the 1:2 ChCl/catechol cocrystal significantly deviated from the experimental data (Δ = 38.4%). As can be seen in Figure 4A, the predicted melting enthalpy allowed for a better description of the liquidus and solidus data of the 1:2 ChCl/catechol cocrystal compared to the experimental melting enthalpy.

As previously discussed, it was challenging to interpret the melting enthalpy of the 1:1 ChCl/resorcinol cocrystal from the DSC curve and to crystallize the 1:2 ChCl/resorcinol cocrystal. When the experimental melting enthalpy of 1:1 and 1:2 ChCl/resorcinol cocrystals was used to calculate the liquidus line of the cocrystals in the ChCl/resorcinol system (Figure 4B), no physical solution could be obtained. In contrast, the calculated melting enthalpy of both cocrystals allowed for the prediction of the liquidus and solidus data of the cocrystals. Thus, despite a significant deviation between the predicted and experimental melting enthalpy of 1:1 and 1:2 ChCl/resorcinol cocrystals, the former could be considered more reliable than those estimated experimentally. Similarly, in the ChCl/hydroquinone system (Figure 4C), the liquidus and solidus temperatures calculated using the predicted melting enthalpy of the 1:1 ChCl/hydroquinone cocrystal were in a better agreement with the experimental SLE data compared to those obtained using the experimental melting enthalpy.

Cocrystal formation in the ChCl/urea system has been controversial. Morrison et al.[35] hinted at the 1:2 ChCl/urea cocrystal using PXRD measurements. Van den Bruinhorst et al.[36] provided further evidence regarding the 1:2 ChCl/urea cocrystal formation. The SLE data of samples prepared by grinding pure solid ChCl and urea or crystallized 1:2 molar ratio mixture and pure urea were different. This indicates that the crystallized 1:2 molar ratio sample is not a mixture of ChCl and urea but rather a new solid phase. However, it was claimed that any slight change in the molar ratio between the constituents could hinder the cocrystal formation. In this work, PXRD measurements for the ChCl/urea system across the entire composition range of the system showed the formation of the 1:2 ChCl/urea (see Figure S2 in the Electronic Supporting Information). Thus, the 1:2 ChCl/urea cocrystal is stable despite the kinetically hindered crystallization. The kinetic limitation in crystallizing the 1:2 ChCl/urea cocrystal could lead to underestimating the melting enthalpy of the cocrystal. As can be seen in Figure 4D, the liquidus line of the 1:2 ChCl/urea cocrystal exists over a small composition range. Moreover, the two solidus temperatures of the system were not far from the melting temperature of the cocrystal. Thus, it was difficult to confirm the reliability of either the predicted or the experimental melting enthalpy of the cocrystal. In conclusion, despite the large deviation observed between experimental and predicted melting enthalpy values, the calculated liquidus line of the studied cocrystals using the predicted melting enthalpy was in similar or better agreement with the experimental SLE data compared to using the experimentally determined melting enthalpy of the cocrystal.

3.2. Systems with Unknown Cocrystal Melting Enthalpy. The SLE phase diagram of several eutectic systems was reported in the literature without a detailed investigation of the formed solid phases. In some systems, cocrystal

https://doi.org/10.1021/acs.cgd.4c00393
Cryst. Growth Des. 2024, 24, 4770−4780

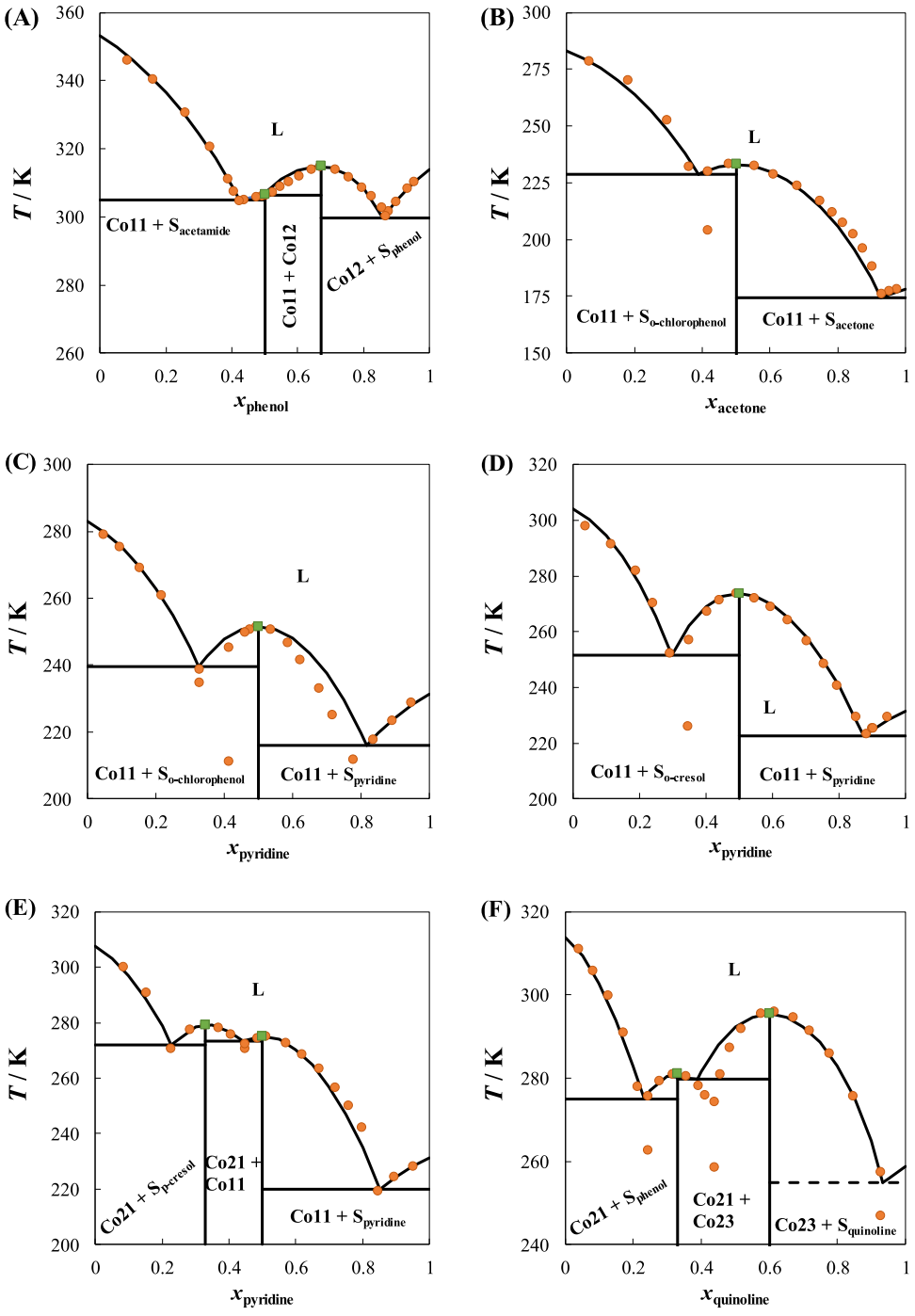

Figure 5. Solid−liquid phase diagram of (A) acetamide/phenol,[5,38] (B) *o*-chlorophenol/acetone,[39] (C) *o*-chlorophenol/pyridine,[39] (D) *o*-cresol/pyridine,[39] (E) *p*-cresol/pyridine,[39] and (F) phenol/quinolone.[39] Legend: ● (orange) liquidus data and ■ (green) cocrystal; —— NRTL.

formation was speculated from the course of SLE data. However, no information was available regarding the melting temperature, melting enthalpy, and stoichiometry of the cocrystals. Accordingly, modeling SLE in such systems was not possible. In this section, 6 binary eutectic systems in which cocrystal formation was not investigated extensively but only speculated from the measured SLE data were considered. The stoichiometry and melting temperature of the formed cocrystals could be assumed according to the course of the SLE data in the middle section of the phase diagram. In contrast, the cocrystal melting enthalpy could not be obtained directly from SLE measurements. For instance, Tumakaka et al.[5] found that the only approach to accurately model the SLE data of cocrystals with unknown melting enthalpy is by fitting the experimental SLE data of the cocrystal liquidus line to obtain its melting enthalpy. Nevertheless, the proposed approach in this work could estimate the melting enthalpy of the formed cocrystals without the need to fit the cocrystal liquidus data. Accordingly, the SLE data of the cocrystal could be predicted.

The SLE phase diagram of 6 different eutectic systems with cocrystal formation was modeled without information regarding stoichiometry and melting properties of the cocrystals. The stoichiometry and melting temperature of the

https://doi.org/10.1021/acs.cgd.4c00393
Cryst. Growth Des. 2024, 24, 4770−4780

cocrystals were speculated from the course of SLE data. The proposed approach was used to estimate the melting enthalpy of the cocrystals (see Table S8 in the Electronic Supporting Information). Figure 5 shows the phase diagram of 6 binary eutectic systems modeled using the NRTL and the calculated cocrystal melting enthalpy. As can be seen in Figure 5A, the SLE phase diagram of the acetamide/phenol system was successfully modeled using the predicted melting enthalpy of the cocrystals. Similarly, the calculated liquidus lines of the *o*-chlorophenol/acetone (Figure 5B), *o*-cresol/pyridine (Figure 5D), and *p*-cresol/pyridine (Figure 5E) systems were in good agreement with the experimental SLE data across the entire composition range of the system. On the other hand, the calculated 1:1 cocrystal liquidus line in the *o*-chlorophenol/pyridine (Figure 5C) slightly deviated from the experimental SLE data, indicating that the predicted cocrystal melting enthalpy was overestimated. It is worth mentioning that for the phenol/quinoline system, the SLE data of the 2:3 cocrystal was used to obtain the NRTL binary interaction parameters of the system. This was necessary as no liquidus data were available for quinoline. Fitting only phenol liquidus data to obtain the NRTL model parameters might not allow for a good description of the system's nonideality. Nevertheless, the liquidus line of the 2:1 cocrystal was well predicted using the calculated melting enthalpy of the cocrystal. In conclusion, the proposed approach in this work allowed for the prediction of the SLE phase diagram of eutectic systems with cocrystal formation even without a detailed experimental investigation of the formed cocrystals.

4. CONCLUSIONS

A thermodynamic approach was proposed in this work to estimate the melting enthalpy of cocrystals. The solid phase of the cocrystal was assumed to be a conjunction of units of the pure constituents with their respective stoichiometric ratio in the cocrystal. On the other hand, the liquid melt of the cocrystal is a solution of the two constituents. The enthalpy change of the cocrystal melting process was calculated using the melting properties of pure components, the stoichiometry of the cocrystal, the cocrystal melting temperature, and the enthalpy of mixing.

The proposed approach was applied to 15 cocrystals of 10 binary eutectic systems. The predicted melting enthalpy of the cocrystals largely deviated from the experimental ones in some cases; however, modeling the liquidus lines of cocrystals in the binary eutectic systems showed that the calculated melting enthalpy provided more reliable predictions for the solubility of the cocrystal. This was particularly the case when experimentally obtaining the cocrystal melting enthalpy was challenging.

Although no experimental investigations were performed to determine the melting properties and stoichiometry of the cocrystals in some systems, the cocrystal stoichiometry and melting temperature could be estimated from the course of SLE data, which were sufficient to predict the cocrystal melting enthalpy using the proposed approach in this work. Accordingly, the complete SLE phase diagram of these mixtures was modeled accurately. The advantage of the proposed approach is the ability to model the SLE phase diagram of eutectic systems without requiring extensive investigations of the cocrystal stoichiometry and melting properties, especially when crystallizing the cocrystal is challenging. Combining our approach with a predictive thermodynamic model could represent an efficient strategy for cocrystal design and screening.

■ ASSOCIATED CONTENT

Data Availability Statement

The data that support the findings of this study are available within the article and Supporting Information.

Supporting Information

The Supporting Information is available free of charge at https://pubs.acs.org/doi/10.1021/acs.cgd.4c00393.

List of systems considered in this work and their cocrystals' melting temperature and stoichiometry; pure components' melting properties and constant pressure heat capacity; NRTL binary interaction parameters of studied systems; DSC and PXRD measurement details; SLE data of ChCl/resorcinol and nicotinamide/glutaric acid; PXRD patterns of samples in ChCl/resorcinol, ChCl/urea, and nicotinamide/glutaric acid; DSC curves of 1:1 and 1:2 ChCl/resorcinol cocrystals; and calculated melting enthalpy of studied cocrystals (PDF)

■ AUTHOR INFORMATION

Corresponding Author

Ahmad Alhadid − *Biothermodynamics, TUM School of Life Sciences, Technical University of Munich, Freising 85354, Germany*; orcid.org/0000-0003-1443-1517; Email: ahmad.alhadid@tum.de

Authors

Lea Kefalianakis − *Biothermodynamics, TUM School of Life Sciences, Technical University of Munich, Freising 85354, Germany*

Alexander Wendler − *Biothermodynamics, TUM School of Life Sciences, Technical University of Munich, Freising 85354, Germany*

Sahar Nasrallah − *Biothermodynamics, TUM School of Life Sciences, Technical University of Munich, Freising 85354, Germany*

Christian Jandl − *Department of Chemistry, TUM School of Natural Sciences, Technical University of Munich, Garching 85748, Germany*

Silva M. Kronawitter − *Department of Chemistry, TUM School of Natural Sciences, Technical University of Munich, Garching 85748, Germany*; orcid.org/0000-0001-7421-6152

Gregor Kieslich − *Department of Chemistry, TUM School of Natural Sciences, Technical University of Munich, Garching 85748, Germany*; orcid.org/0000-0003-2038-186X

Mirjana Minceva − *Biothermodynamics, TUM School of Life Sciences, Technical University of Munich, Freising 85354, Germany*; orcid.org/0000-0001-9820-7410

Complete contact information is available at: https://pubs.acs.org/10.1021/acs.cgd.4c00393

Author Contributions

Ahmad Alhadid contributed to conceptualization, methodology, validation, formal analysis, investigation, data curation, supervision, and writing—original draft; **Lea Kefalianakis** contributed to formal analysis, investigation, and data curation; **Alexander Wendler** contributed to investigation and data curation; **Sahar Nasrallah** contributed to validation, formal

https://doi.org/10.1021/acs.cgd.4c00393
Cryst. Growth Des. 2024, 24, 4770−4780

analysis, investigation, and data curation; **Christian Jandl** contributed to formal analysis, investigation, and data curation; **Silva M. Kronawitter** contributed to formal analysis, investigation, and data curation; **Gregor Kieslich** contributed to writing—review and editing and supervision; and **Mirjana Minceva** contributed to writing—review and editing, resources, and supervision.

Notes

The authors declare no competing financial interest.

REFERENCES

(1) Gamsjäger, H.; Lorimer, J. W.; Scharlin, P.; Shaw, D. G. Glossary of terms related to solubility (IUPAC Recommendations 2008). *Pure Appl. Chem.* **2008**, *80*, 233−276.

(2) Prausnitz, J. M.; Lichtenthaler, R. N.; de Azevedo, E. G. *Molecular Thermodynamics of Fluid-phase Equilibria*; Prentice Hall PTR, 1999; .

(3) Couillaud, B. M.; Espeau, P.; Mignet, N.; Corvis, Y. State of the Art of Pharmaceutical Solid Forms: from Crystal Property Issues to Nanocrystals Formulation. *ChemMedChem* **2019**, *14* (1), 8−23.

(4) Jones, W.; Motherwell, W. D. S.; Trask, A. V. Pharmaceutical Cocrystals: An Emerging Approach to Physical Property Enhancement. *MRS Bull.* **2006**, *31* (11), 875−879.

(5) Tumakaka, F.; Prikhodko, I. V.; Sadowski, G. Modeling of solid-liquid equilibria for systems with solid-complex phase formation. *Fluid Phase Equilib.* **2007**, *260* (1), 98−104.

(6) Lange, L.; Sadowski, G. Thermodynamic Modeling for Efficient Cocrystal Formation. *Cryst. Growth Des.* **2015**, *15* (9), 4406−4416.

(7) Alhadid, A.; Jandl, C.; Mokrushina, L.; Minceva, M. Cocrystal Formation in Choline Chloride Deep Eutectic Solvents. *Cryst. Growth Des.* **2022**, *22* (3), 1933−1942.

(8) Lange, L.; Heisel, S.; Sadowski, G. Predicting the Solubility of Pharmaceutical Cocrystals in Solvent/Anti-Solvent Mixtures. *Molecules* **2016**, *21* (5), 593.

(9) Lange, L.; Sadowski, G. Polymorphs, Hydrates, Cocrystals, and Cocrystal Hydrates: Thermodynamic Modeling of Theophylline Systems. *Cryst. Growth Des.* **2016**, *16* (8), 4439−4449.

(10) Wolbert, F.; Brandenbusch, C.; Sadowski, G. Selecting Excipients Forming Therapeutic Deep Eutectic Systems-A Mechanistic Approach. *Mol. Pharmaceutics* **2019**, *16* (7), 3091−3099.

(11) Lohmann, J.; Joh, R.; Gmehling, J. Estimation of Enthalpies of Fusion, Melting Temperatures, Enthalpies of Transition, and Transition Temperatures of Pure Compounds from Experimental Binary Solid-Liquid Equilibrium Data of Eutectic Systems. *J. Chem. Eng. Data* **1997**, *42* (6), 1176−1180.

(12) Alhadid, A.; Jandl, C.; Mokrushina, L.; Minceva, M. Cocrystal Formation in l-Menthol/Phenol Eutectic System: Experimental Study and Thermodynamic Modeling. *Cryst. Growth Des.* **2022**, *22* (6), 3973−3980.

(13) Alhadid, A.; Jandl, C.; Mokrushina, L.; Minceva, M. Nonideality and cocrystal formation in l-menthol/xylenol eutectic systems. *J. Mol. Liq.* **2022**, *367*, 120582.

(14) Alhadid, A.; Luca, S. V.; Nasrallah, S.; Minceva, M. Experimental investigation and thermodynamic modeling of cannabidiol solubility in plant oils and hydrophobic eutectic systems. *J. Mol. Liq.* **2023**, *372*, 121172.

(15) Teixeira, G.; Abranches, D. O.; Ferreira, O.; Coutinho, J. A. P. Estimating the Melting Temperatures of Type V Deep Eutectic Solvents. *Ind. Eng. Chem. Res.* **2023**, *62* (36), 14638−14647.

(16) Loschen, C.; Klamt, A. Cocrystal Ternary Phase Diagrams from Density Functional Theory and Solvation Thermodynamics. *Cryst. Growth Des.* **2018**, *18* (9), 5600−5608.

(17) Cappuccino, C.; Cusack, D.; Flanagan, J.; Harrison, C.; Holohan, C.; Lestari, M.; Walsh, G.; Lusi, M. How Many Cocrystals Are We Missing? Assessing Two Crystal Engineering Approaches to Pharmaceutical Cocrystal Screening. *Cryst. Growth Des.* **2022**, *22* (2), 1390−1397.

(18) Issa, N.; Karamertzanis, P. G.; Welch, G. W. A.; Price, S. L. Can the Formation of Pharmaceutical Cocrystals Be Computationally Predicted? I. Comparison of Lattice Energies. *Cryst. Growth Des.* **2009**, *9* (1), 442−453.

(19) Karamertzanis, P. G.; Kazantsev, A. V.; Issa, N.; Welch, G. W. A.; Adjiman, C. S.; Pantelides, C. C.; Price, S. L. Can the Formation of Pharmaceutical Cocrystals Be Computationally Predicted? 2. Crystal Structure Prediction. *J. Chem. Theory Comput.* **2009**, *5* (5), 1432−1448.

(20) Rama Krishna, G.; Ukrainczyk, M.; Zeglinski, J.; Rasmuson, Å. C. Prediction of Solid State Properties of Cocrystals Using Artificial Neural Network Modeling. *Cryst. Growth Des.* **2018**, *18* (1), 133−144.

(21) Alhadid, A.; Jandl, C.; Nasrallah, S.; Kronawitter, S. M.; Mokrushina, L.; Kieslich, G.; Minceva, M. Estimating the nonideality of eutectic systems containing thermally unstable substances. *J. Chem. Phys.* **2023**, *159* (9), 094503.

(22) Alhadid, A.; Jandl, C.; Mokrushina, L.; Minceva, M. Experimental Investigation and Modeling of Cocrystal Formation in L-Menthol/Thymol Eutectic System. *Cryst. Growth Des.* **2021**, *21* (11), 6083−6091.

(23) Zhang, S.-W.; Harasimowicz, M. T.; de Villiers, M. M.; Yu, L. Cocrystals of Nicotinamide and (R)-Mandelic Acid in Many Ratios with Anomalous Formation Properties. *J. Am. Chem. Soc.* **2013**, *135* (50), 18981−18989.

(24) Svärd, M.; Ahuja, D.; Rasmuson, Å. C. Calorimetric Determination of Cocrystal Thermodynamic Stability: Sulfamethazine-Salicylic Acid Case Study. *Cryst. Growth Des.* **2020**, *20* (7), 4243−4251.

(25) Demirel, Y.; Gecegörmez, H. Simultaneous representation of excess enthalpy and vapor-liquid equilibrium data by the NRTL and UNIQUAC models. *Fluid Phase Equilib.* **1991**, *65*, 111−133.

(26) van den Bruinhorst, A.; Avila, J.; Rosenthal, M.; Pellegrino, A.; Burghammer, M.; Costa Gomes, M. Defying decomposition: the curious case of choline chloride. *Nat. Commun.* **2023**, *14* (1), 6684.

(27) Lobo Ferreira, A. I. M. C.; Vilas-Boas, S. M.; Silva, R. M. A.; Martins, M. A. R.; Abranches, D. O.; Soares-Santos, P. C. R.; Almeida Paz, F. A.; Ferreira, O.; Pinho, S. P.; Santos, L. M. N. B. F.; et al. Extensive characterization of choline chloride and its solid-liquid equilibrium with water. *Phys. Chem. Chem. Phys.* **2022**, *24* (24), 14886−14897.

(28) Jamróz, M. E.; Palczewska-Tulińska, M.; Wyrzykowska-Stankiewicz, D.; Szafrański, A. M.; Polaczek, J.; Dobrowolski, J. C.; Jamróz, M. H.; Mazurek, A. P. The urea-phenol(s) systems. *Fluid Phase Equilib.* **1998**, *152* (2), 307−326.

(29) Dobrowolski, J.; Jamróz, M. H.; Jamróz, M.; Wyrzykowska-Stankiewicz, D.; Szafrański, A. M.; Polaczek, J. Infrared, cryometric and calorimetric studies on the urea-phenol system. *J. Mol. Struct.* **1988**, *175*, 227−232.

(30) Meng, X.; Ballerat-Busserolles, K.; Husson, P.; Andanson, J.-M. Impact of water on the melting temperature of urea + choline chloride deep eutectic solvent. *New J. Chem.* **2016**, *40* (5), 4492−4499.

(31) Cysewski, P.; Przybyłek, M.; Kowalska, A.; Tymorek, N. Thermodynamics and Intermolecular Interactions of Nicotinamide in Neat and Binary Solutions: Experimental Measurements and COSMO-RS Concentration Dependent Reactions Investigations. *Int. J. Mol. Sci.* **2021**, *22* (14), 7365.

(32) van den Bruinhorst, A.; Kollau, L. J. B. M.; Vis, M.; Hendrix, M. M. R. M.; Meuldijk, J.; Tuinier, R.; Esteves, A. C. C. From a eutectic mixture to a deep eutectic system via anion selection: Glutaric acid + tetraethylammonium halides. *J. Chem. Phys.* **2021**, *155* (1), 014502.

(33) Steele, W. V.; Chirico, R. D.; Cowell, A. B.; Knipmeyer, S. E.; Nguyen, A. Thermodynamic Properties and Ideal-Gas Enthalpies of Formation for 1,4-Diisopropylbenzene, 1,2,4,5-Tetraisopropylbenzene, Cyclohexanone Oxime, Dimethyl Malonate, Glutaric Acid, and Pimelic Acid. *J. Chem. Eng. Data* **2002**, *47* (4), 725−739.

(34) Martins, M. A. R.; Pinho, S. P.; Coutinho, J. A. P. Insights into the Nature of Eutectic and Deep Eutectic Mixtures. *J. Solution Chem.* **2019**, *48* (7), 962−982.

https://doi.org/10.1021/acs.cgd.4c00393
Cryst. Growth Des. 2024, 24, 4770−4780

(35) Morrison, H. G.; Sun, C. C.; Neervannan, S. Characterization of thermal behavior of deep eutectic solvents and their potential as drug solubilization vehicles. *Int. J. Pharm.* **2009**, *378* (1−2), 136−139.
(36) van den Bruinhorst, A.; Kollau, L. J. B. M.; Kroon, M. C.; Meuldijk, J.; Tuinier, R.; Esteves, A. C. C. A centrifuge method to determine the solid-liquid phase behavior of eutectic mixtures. *J. Chem. Phys.* **2018**, *149* (22), 224505.
(37) Silva, L. P.; Araújo, C. F.; Abranches, D. O.; Melle-Franco, M.; Martins, M. A. R.; Nolasco, M. M.; Ribeiro-Claro, P. J. A.; Pinho, S. P.; Coutinho, J. A. P. What a difference a methyl group makes - probing choline-urea molecular interactions through urea structure modification. *Phys. Chem. Chem. Phys.* **2019**, *21* (33), 18278−18289.
(38) Walas, S. M. *Phase Equilibria in Chemical Engineering*; Butterworth-Heinemann, 2013; .
(39) Bramley, A. XXXVII.—The study of binary mixtures. Part III. Freezing-point curves. *J. Chem. Soc., Trans.* **1916**, *109*, 469−496.

https://doi.org/10.1021/acs.cgd.4c00393
Cryst. Growth Des. 2024, 24, 4770−4780